COMPARISON AMONG BUTTERWORTH, HANN AND GAUSSIAN FILTER IN ACCURATE ACTIVITY QUANTIFICATION OF 99mTc SPECT/CT IMAGING

NADHRAH BINTI SALIMMI

SCHOOL OF HEALTH SCIENCES UNIVERSITI SAINS MALAYSIA

2025

COMPARISON AMONG BUTTERWORTH, HANN AND GAUSSIAN FILTER IN ACCURATE ACTIVITY QUANTIFICATION OF $^{99\mathrm{m}}$ TC SPECT/CT IMAGING

By
NADHRAH BINTI SALIMMI
Dissertation submitted in partial fulfilment of the requirements for the degree of Bachelor in Medical Radiation

June 2025

CERTIFICATE

This is to certify that the dissertation entitled "COMPARISON AMONG BUTTERWORTH, HANN AND GAUSSIAN FILTER IN ACCURATE ACTIVITY QUANTIFICATION OF ^{99m}TC SPECT/CT IMAGING" is the bona fide record of research work done NADHRAH BINTI SALIMMI during the period from October 2024 to June 2025 under my supervision. I have read this dissertation and that in my opinion it conforms to acceptable standards of scholarly presentation and is fully adequate, in scope and quality, as a dissertation to be submitted in partial fulfillment for the degree of Bachelor in Medical Radiation.

Supervisor,	Co-supervisor,
Dr. Mariamie binti Mussaruddin	Dr. Mohammad Khairul Azhar Abdul Razab
University Lecturer,	University Lecturer,
School of Health Sciences Health Campus	School of Health Sciences Health Campus
Universiti Sains Malaysia,	Universiti Sains Malaysia,
16150 Kubang Kerian Kelantan, Malaysia	16150 Kubang Kerian Kelantan, Malaysia

Date: June 2025

Date: June 2025

DECLARATION

I hereby declare that this dissertation is the result of my own investigations, except where

otherwise stated and duly acknowledged. I also declare that it has not been previously or

concurrently submitted as a whole for any other degrees at Universiti Sains Malaysia or other

institutions. I grant Universiti Sains Malaysia the right to use the dissertation for teaching,

research, and promotional purposes.

NADHRAH BINTI SALIMMI

Date: June 2025

iv

ACKNOWLEDGEMENT

First and foremost, I would like to express my gratitude to Allah Almighty for His blessings and the strength He gave me throughout my research journey. All praise is due to Allah for allowing me to successfully complete this study. To start with, I would like to express my sincere thanks to my supervisor, Dr. Marianie binti Musaruddin from the School of Health Sciences, Universiti Sains Malaysia (USM) for her constant guidance, advice, and support throughout this research. Her help was crucial during both the experimental and writing parts of my thesis. This thesis would not have been possible without her valuable suggestions despite of her busy schedule. The quality of this study has been much improved by her careful attention to detail and commitment to high standards. I also want to express my gratitude to Dr. Mohammad Khairul Azhar Abdul Razab, my co-supervisor for his efforts and willingness to take the time to address my questions whenever my supervisor was uncertain have been greatly appreciated. Without his encouragement, I would not have been able to complete my dissertation on time.

In addition, I would want to use this chance to express my gratitude to my field supervisor, Encik Ahamad Thaifur bin Khaizul who helped with source preparation and managing the gamma camera. The data collection part of this study would not have been complete without his support because he was a big assistance and mentor when it came to carrying out the experiment for the study.

Finally, I would like to express my heartfelt gratitude to my fellow friends, parents and family for their love, care and support. Their encouragement has been a constant source of strength throughout my life and the completion of this study.

Table of Contents

CERT	IFICATEiii
DECL	ARATIONiv
ACKN	OWLEDGEMENTv
LIST C	OF TABLESix
LIST (OF FIGURESx
LIST (DF SYMBOLSxii
LIST (OF ABBREVIATIONSxiii
ABSTI	RAKxv
ABSTI	RACTxvi
СНАР	ΓER 11
INTRO	DUCTION1
1.1	Background of Study
1.2	Problem Statement
1.3	Aim of Study5
1.4	Research Objectives5
1.5	Significance of Study6
СНАР	ΓER 27
LITER	ATURE REVIEW7

2.1 Ov	verview of Nuclear Medicine Imaging	7
2.1.1	Technetium-99m (^{99m} TC) radionuclide	8
2.2 Ga	umma Camera (SPECT/CT)	9
2.3 SI	PECT/CT reconstruction	10
2.3.1	Filter Back Projection (FBP)	11
2.3.2	Ordered Subsets Expectation Maximization (OSEM)	11
2.3.3	Effects of different filter used	12
2.4 Ac	ctivity quantification of SPECT/CT	15
2.4.1	Calibration Factor (CF)	16
2.4.2	Partial Volume Effect (PVE)	17
2.4.3	Recovery Coefficient (RC)	18
2.4.4	Spatial resolution	20
CHAPTER	3	22
METHOD	OLOGY	22
3.1 Mater	ial	22
3.1.1	Discovery NM/CT 670 Pro SPECT/CT	22
3.1.2	NEMA 2007/IEC 2008 phantom	23
3.1.3	Petri dish for calibration	25
3.1.4	Unsealed source Technetium-99m (^{99m} Tc)	26
	Onscaled source Technicidin-95iii (Tej	∠0
3.1.5	Dose Calibrator	
3.1.5 3.1.6	· · ·	27
	Dose Calibrator	27
3.1.6	Dose Calibrator	27 28

3.2	Calibration factor using petri dish	31
3.2	Preparation of NEMA 2007/IEC 2008 phantom	34
3.2	2.3 SPECT/CT Imaging	38
3.2	2.4 SPECT/CT Image Reconstruction and Segmentation	39
3.2	Quantitative Analysis of RC with PVC and without PVC	41
СНАР	TER 4	43
RESUI	LT AND DISCUSSION	43
4.1	SPECT/CT Image Reconstruction	43
4.2	Evaluation of Recovery Coefficient (RC)	46
4.3	Quantification error with PVC and without PVC	51
СНАР	TER 5	58
CONC	LUSION	58
5.1	Conclusion	58
5.2	Limitation of Study	58
5.3	Recommendation for Future Research	59
REFEI	RENCES	60
APPEN	NDICES	64
Арре	endix A	64
Appe	endix B	67

LIST OF TABLES

Table 3.1	The dimension of NEMA phantom used in this study	
Table 3.2	The detailed dimension of six spherical shapes in NEMA phantom	25
Table 3.3	Key parameters for planar imaging during image acquisition.	33
Table 3.4	Total activity required for each TBR 10:1 and TBR 5	36
Table 3.5	Actual activity and activity concentration for each sphere of TBR 10:1	
Table 3.6	Actual activity and activity concentration for each sphere of TBR 5:1	
Table 3.7	Imaging protocol for CT and SPECT	39
Table 4.1	Result of the image reconstruction for Hann, Butterworth and Gaussian	43 – 45
	filter with different parameters	
Table 4.2	Recovery coefficient (RC) value of Hann filter with different parameters	49
	for TBR 10:1	
Table 4.3	Recovery coefficient (RC) value of Butterworth filter with different	50
	parameters for TBR 10:1	
Table 4.4	Recovery coefficient (RC) value of Gaussian filter with different	
	parameters for TBR 10:1	

LIST OF FIGURES

Figure 2.1	Schematic overview of the ⁹⁹ Mo/ ^{99m} Tc generator system 9	
Figure 3.1	GE Discovery NM/CT 670 Pro SPECT/CT at HPUSM	
Figure 3.2	NEMA 2007/IEC 2008 phantom	
Figure 3.3	Petri dish used for sensitivity of ^{99m} Tc SPECT/CT	
Figure 3.4	The dose calibrator at the dispensing room was shielded with L-block	
	shield	
Figure 3.5	50-cc syringe and plastic tube	28
Figure 3.6	Xeleris Functional Imaging Workstation Ver.3.1	29
Figure 3.7	Summary of the process of analyzing accuracy on activity quantification	31
	using different filter parameters	
Figure 3.8	(a) The preparation of petri dish filled with 99mTc (b) The dilution of	32
	^{99m} Tc inside 20 ml of distilled water (c) The measurement of 10 cm	
	distance between LEHR collimator of Detector 1 and petri dish	
Figure 3.9	ROI is drawn to yield total counts of entire volume and background	33
Figure 3.10	Figure 3.10: (a) The preparation of ^{99m} Tc b) 99mTc diluted and filled	37 - 38
	inside the background of the phantom (c) 99mTc was filled into the	
	spheres using a 50-cc syringe with plastic tube. (d) NEMA phantom that	
	shielded with L-block shield to prevent unwanted radiation to personnel	
	while carrying the phantom to SPECT/CT room for scanning	
Figure 3.11	The arrangement of NEMA phantom position on table couch for image	39
	acquisition	
Figure 3.12	The coronal, sagittal and transaxial view of images	40

Figure 3.13	3 (a) The segmentation of all six spheres (b) The segmentation of six	
	VOIs in the background.	
Figure 4.1	Graph Recovery coefficient (RC) as a function of spherical diameter	47
	for an image reconstructed using the Hann filter	
Figure 4.2	Graph Recovery coefficient (RC) as a function of spherical diameter	48
	for an image reconstructed using the Butterworth filter	
Figure 4.3	Graph Recovery coefficient (RC) as a function of spherical diameter	48
	for an image reconstructed using the Gaussian filter	
Figure 4.4	Graph of quantification error across spherical diameters for both with	51 – 52
	and without PVC, using the Hann filter with a) a COF of 0.3 b) a COF	
	of 0.5 c) a COF of 0.9	
Figure 4.5	Graph of quantification error across spherical diameters for both with	53 – 54
	and without PVC, using the Butterworth filter with a) a COF of 0.2 b)	
	a COF of 0.5 c) a COF of 0.9	
Figure 4.6	Figure 4.6: Graph of quantification error across spherical diameters for	54 - 55
	both with and without PVC, using the Gaussian filter with a) a FWHM	
	of 1 mm b) a FWHM of 4 mm c) a FWHM of 7 mm	

LIST OF SYMBOLS

% Percentage Ao **Initial Activity** $T_{1/2}$ Half life ^{99m}Tc Technetium-99m ⁹⁹Mo Molybdenum-99 99mTc-MDP Technetium 99m-methyl diphosphonate ^{99m}Tc-sestamibi Technetium 99m-sestamibi 99mTc-MAG3 Tc-99m-mercaptoacetyltriglycine ¹⁷⁷LU Luthenium-177 Α Activity of radionuclide Kilobecquerel kBq Kilovolt peak kVp MBq Megabecquerel Millicurie mCi Millilitre ml N Mean Count Time of Acquisition t $CuAl_2$ Copper Aluminide NaTcO₄-Sodium pertechnetate (NaTcO₄-) Volume vol λ Decay constant

LIST OF ABBREVIATIONS

EANM European Association of Nuclear Medicine

ROI Region of Interest

3D 3-Dimensional

CT Computed Tomography

GE General Electric

HPUSM Hospital Pakar Universiti Sains Malaysia

mA Milliampere

mAs Milliampere-second

NEMA National Electrical Manufacturers Association

CF Calibration Factor

NM Nuclear Medicine

OSEM Ordered Subset Expectation Maximisation

PET Positron Emission Tomography

PVC Partial Volume Correction

PVE Partial Volume Effect

FBP Filter back projection

RC Recovery Coefficient

SNR Signal to Noise Ratio

SPECT Single Photon Emission Computed Tomography

cps Count per second

MRI Magnetic Resonance Imaging

TBR Tumor to Background ratio

VOI Volume of Interest

AC Attenuation Correction

NC Non-attenuation Correction

CTAC CT-Based Attenuation Correction

MLEM Maximum Likelihood Expectation Maximization

LEHR Low Energy High Resolution

CNR Contrast-to-Noise ratio

SUV Standardized Uptake Value

PERBANDINGAN ANTARA PENAPIS BUTTERWORTH, HANN DAN GAUSSIAN TERHADAP KETEPATAN AKTIVITI KUANTIFIKASI PENGIMEJAN 99mTC SPECT/CT.

ABSTRAK

Kajian ini memberi tumpuan terhadap penilaian ketepatan kuantifikasi aktiviti terhadap pengimejan Technetium-99m (99mTc) Pancaran Foton Tunggal Tomografi Berkomputer / Tomografi Berkomputer (SPECT/CT) yang dicapai melalui tiga penapis, iaitu penapis Butterworth, Gaussian dan Hann dengan parameter yang berbeza. Objektif utama adalah untuk menentukan penapis dan parameter yang optimum terhadap kuantifikasi aktiviti ^{99m}Tc yang tepat dalam pengimejan SPECT. Pengimejan kuantitatif dengan ^{99m}Tc SPECT/CT menghadapi cabaran seperti bunyi, kekangan resolusi dan kesan volum separa. Oleh itu, penapis digunakan untuk meningkatkan resolusi dan mengurangkan bunyi bagi ketepatan diagnostik yang lebih baik. Kajian ini menggunakan fantom NEMA 2007/IEC 2008 yang diisi dengan 99mTc menggunakan sistem GE Discovery NM/CT 670 Pro SPECT/CT dan nisbah tumor-ke-latar belakang (TBR) ialah 5:1 dan 10:1. Eksperimen ini melibatkan pengimbasan menggunakan tiga parameter penapis dan melakukan perbandingan terperinci hasil menggunakan pekali pemulihan (RC) untuk menilai prestasi penapis merentasi pelbagai saiz sfera. Kalibrasi sensitiviti terlebih dahulu dilakukan menggunakan kepekatan aktiviti (AC) 30 kBq/ml untuk menetapkan faktor kalibrasi (CF) terhadap kuantifikasi aktiviti 99mTc SPECT yang merupakan langkah penting untuk memastikan ketepatan hasil diagnostik. Kemudian, pembinaan imej dan kuantifikasi dilakukan menggunakan perisian *OMetrix* dan workstation Xeleris bagi memudahkan analisis terperinci. Berdasarkan kajian, penapis Butterworth dengan frekuensi potongan 0.5 (COF) memberikan prestasi yang paling optimum di pelbagai diameter sfera dan menghasilkan kesilapan kuantifikasi purata yang paling kecil apabila digunakan dengan pembetulan isipadu sebahagian (PVC).

COMPARISON BETWEEN BUTTERWORTH, HANN AND GAUSSIAN FILTER IN ACCURATE ACTIVITY QUANTIFICATION OF 99mTC SPECT/CT IMAGING

ABSTRACT

This study focuses on evaluating the accuracy of activity quantification in ^{99m}Tc Single Photon Emission Computed Tomography/Computed Tomography (SPECT/CT) imaging achieved through three different filters which is Butterworth, Gaussian and Hann filters with different parameters. The primary objective is to determine the optimal filter with optimal parameter for accurate quantification of 99mTc activity in SPECT/CT imaging. Quantitative imaging with ^{99m}Tc SPECT/CT faces challenges such as noise, resolution limitations and partial volume effects. Therefore, filters are applied to improve resolution and reduce noise for better diagnostic accuracy. The study utilizes NEMA 2007/IEC 2008 phantoms filled with ^{99m}Tc, using the GE Discovery NM/CT 670 Pro SPECT/CT system and tumor-to-background ratios (TBR) of 5:1 and 10:1. The experiment involved scanning with three filter parameters and performing a thorough comparison of the results using the recovery coefficient (RC) to evaluate filter performance across different sphere sizes. The sensitivity calibration was performed first using an activity concentration (AC) of 30 kBq/ml to establish the calibration factor (CF) for ^{99m}Tc SPECT activity quantification which is a crucial step in ensuring the accuracy of the diagnostic results. Then, image reconstruction and quantification were carried out using QMetrix software and the Xeleris workstation to facilitate detailed analysis. Based on the findings, Butterworth filter with a cut-off frequency (COF) of 0.5 provided the most optimal performance across various spherical diameters and yielded the smallest average quantification error when applied with Partial Volume Correction (PVC).

CHAPTER 1

INTRODUCTION

1.1 Background of Study

Nuclear medicine relies heavily on gamma (γ) ray imaging from radionuclides to detect and stage various diseases, including myocardial perfusion, bone cancer, and thyroid disease. Single Photon Emission Computed Tomography (SPECT) is a commonly used imaging modality that offers noninvasive visualization of internal structure and function of human body. It uses radiotracers to simulate distribution of a γ -emitter throughout a patient. One of the most used radiopharmaceuticals in SPECT imaging is Technetium-99m (99m Tc), a gamma-emitting isotope that is used due to its favorable half-life and energy characteristics. 99m Tc is an even preferable radionuclide owing to having a half-life of six hours which is suitable for imaging later (Kane & Davis, 2022). It also produces gamma rays with 140 keV energy that are good for detection by SPECT cameras. 99m Tc application is extended to different types of diagnostics as well as the cardiac, brain, and oncology image investigations. The ability to quantify the distribution of 99m Tc within the body allows clinicians to evaluate physiological and pathological conditions, thus aiding in the diagnosis and monitoring of diseases.

However, the quality of SPECT images can be affected by several factors, including photon attenuation and scattering, collimator blurring, partial volume effects (PVEs) and the reconstruction algorithm (Keamogetswe Ramonaheng et al., 2021). These factors are inherent in the imaging process and degrade images from an ideal representation of the imaged object, resulting in inaccuracies in activity quantification, which is critical for accurate clinical assessment. Because of their better quantitative accuracy than planar images, SPECT/CT images have been included into many dosimetry procedures for ^{99m}Tc activity quantification. However, the effects of the above-described degrading elements complicate SPECT imaging. Thus, efforts to compensate for these factors must be taken to improve the quantified activity's accuracy.

Accurate dosimetry is heavily dependent on the accuracy with which activity quantification can be accomplished. To address these issues, image reconstruction techniques are used, and filters are applied during the reconstruction process to improve image quality.

SPECT imaging relies on a series of steps to reconstruct two- or three-dimensional images from the detected gamma photons. The primary challenge in SPECT imaging is the reconstruction of high-quality images that can accurately reflect the distribution of the radiotracer within the body. Various image reconstruction algorithms, such as iterative reconstruction and filtered back projection (FBP) methods. Both of which have advantages and disadvantages. FBP, for example, is fast and computationally efficient but struggles with artifacts and noise in low-count images, whereas iterative techniques such as Ordered Subset Expectation Maximization (OSEM) improve noise management but are computationally intensive (Ahmad Saib et al., 2021). Nowadays, ordered subset expectation maximization (OSEM) schemes are the most common iterative reconstruction algorithms in clinical practice as it is the most successful algorithm to overcome the issue of blurring and high dose of projection data.

After the image was reconstructed by OSEM algorithm, post-reconstruction filtering was performed. The problem of filtering the tomography images is crucial since it has a substantial influence on the final image. Image filtering is an operation applied on pixels of an image. The image suppression process in the presence of noise is a mathematical operation that includes smoothing, edge boosting and resolution restoration (Lyra & Ploussi, 2011). Filters are introduced in the reconstruction which is performed on the frequency domain data. The target of filtering is reducing noise and reinforcing the image's details. The attenuation of high-frequency components of noise in projection images is typically done with the aid of filters. Thus, filters can improve the resolution of an image and also limit the noise degradation. Proper filter selection and appropriate smoothing should be considered to help the doctor in a precise diagnosis and interpretation of the results. Pandey and Malhotra (2004) concluded that the filter

parameters should be normalized before application in clinical environment. A series of filters or a single filter that are adequately normalised can be utilized. However, the choice of an optimal filter or their best parameter to be used in clinical practice is not straightforward, due to the large number of different types of filters used in medical imaging.

The low-pass filters, such as the Butterworth and the Gaussian low-pass filters have been extensively used in the reduction of noise at high-frequencies while preserving details at low frequencies, which corresponding to larger structures. In contrast, the Hann filter, a type of windowing filter, is commonly used to smooth images and suppress artifacts. Since there are different features and settings for each filter that may affect performance, it is necessary to have a comparison of their effectiveness on different datasets.

1.2 Problem Statement

Precise quantification of ^{99m}Tc SPECT imaging is difficult to achieve because of noise and resolution limitations of the modality. This is further complicated since it is necessary to obtain accurate localization of defects, an essential requirement in many medical imaging applications. Noise can mask important information and lack of spatial resolution can lead to inaccurate size and shape measurement of pathology. These restrictions reduce the overall accuracy of quantitative measurements in SPECT imaging, particularly for important clinical applications (Sayed & Ismail, 2020). To overcome these challenges, image synthesis algorithms are used in post-processing in order to remove noise and improve the visibility of structures. These filters include the Butterworth, Gaussian, and Hann filters. Different filters work in different ways and affect contrast, signal-to-noise ratio (SNR) and spatial resolution. This study aims to compare these three filters in terms of their ability to improve quantitative accuracy in ^{99m}Tc SPECT imaging.

The Butterworth filter is a low-pass filter designed to suppress high-frequency noise while preserving the overall structure of the image. It achieves this by allowing lower frequencies

to pass through while attenuating higher frequencies, which are often associated with noise. The Butterworth filter's performance is controlled by its cut-off frequency (COF) and order. The COF determines the threshold frequency above which noise is suppressed, while the filter order influences the sharpness of the transition between preserved and attenuated frequencies. Previous studies from Ahmad Saib et al. carried out that the Butterworth filter's limited effectiveness in enhancing image quality for smaller structures, specifically in high-noise environments. While the filter improved contrast and signal-to-noise ratio (SNR) for larger spheres, it struggled with the smallest sphere, where noise interference caused blurring and unclear edges. The study indicates that, at an optimal cutoff frequency (COF) of 7 cycles/mm, the filter increased contrast and SNR for medium to larger spheres. However, for smaller regions, such as diameter sphere of 10 mm in NEMA phantom, the high noise presence impeded detectability and image clarity. This limitation highlights the Butterworth filter's inability to both suppress noise and enhance spatial resolution simultaneously in all cases, pointing to the need for alternative filtering approaches to improve image clarity across different structure sizes in SPECT imaging.

Another common low-pass filter is the Gaussian filter, which can achieve image smoothing by removing high frequencies. It involves applying a Gaussian function to the frequency components to have a smooth transfer between kept and attenuated frequencies. The Full Width at Half Maximum (FWHM) is the central parameter of the Gaussian filter, that indicates the size of the smoothing. Larger FWHM tend to show a stronger noise reduction at the risk of losing finer structures and smaller FWHM conserves more details but brings more noises (Tsutsui et al., 2018). The Gaussian filter can work better with a high-noise environment than the Butterworth filter, because the former possesses the smoother and slower frequency attenuation. This makes it useful for boosting small structures, because it does not have sharp cutoffs like some of the other filters that can create artifacts. However, since the Gaussian filter is tailored to smoothing, it can reduce contrast in some cases which might not be a desirable effect, and it is less effective for larger structures where emphasis on the preservation of edges is important.

The Hann filter, a windowing filter, is mainly applied to suppress artifacts and enhance image smoothness. The Hann filter weighs across the entire frequency spectrum, minimizing the tendency of many visually inspired techniques such as the Butterworth and Gaussian filters which concentrate on the suppression of high frequency noise (Window Types, 2024). The performance of Hann filter is subject to the window size that specifies the bandwidth of frequencies restricted by the filter. One of the main advantages of the Hann filter is the ability to improve the spatial resolution, without considerable decrease of the SNR. This property makes it suited for the detection of small structures and for identifying irregularities where resolution and noise suppression are important. However, the Hann filter may struggle in high-noise environments, as its balanced approach does not provide as much noise suppression as the Butterworth or Gaussian filters (Sayed & Nasrudin, 2016). Nevertheless, its ability to preserve details and reduce artifacts makes it a valuable tool for improving image quality in SPECT imaging.

1.3 Aim of Study

To determine the optimal filter among Butterworth, Gaussian and Hann for accurate activity quantification in ^{99m}Te SPECT/CT imaging.

1.4 Research Objectives

- 1. To determine the calibration factor (CF) for ^{99m}Tc SPECT/CT activity quantification.
- To determine the optimal filter parameters for accurate activity quantification of ^{99m}Tc SPECT/CT imaging.
- 3. To evaluate the accuracy of activity quantification in ^{99m}Tc SPECT/CT imaging achieved using different filters of Butterworth, Gaussian and Hann filters.

1.5 Significance of Study

The aim of this study is to compare the Butterworth, Hann, and Gaussian filters applied to ^{99m}Tc SPECT imaging in terms of quantitative accuracy, focusing on activity quantification and parameter optimization. The use of recovery coefficients, which represent the ratio between measured and true activity values, is essential for evaluating how effectively each filter preserves quantitative data in SPECT imaging. Accurate quantification of radiotracer distribution is crucial for dosimetry and improving treatment outcomes, as it allows for better prediction of therapy response and prevention of toxicity effects (Bailey & Willowson, 2013). Moreover, recent advancements in reconstruction techniques, including scatter correction and attenuation adjustments, have significantly enhanced the quantitative accuracy of SPECT imaging, making it comparable to PET imaging in certain contexts.

CHAPTER 2

LITERATURE REVIEW

2.1 Overview of Nuclear Medicine Imaging

Nuclear medicine imaging plays an important role in diagnosing and monitoring diseases by utilizing radiopharmaceuticals that help assess the metabolic and physiological functions of organs and tissues in vivo. The primary methods to accurately detect abnormalities are Positron Emission Tomography (PET), Single Photon Emission Computed Tomography (SPECT) and planar imaging. SPECT and PET provide more detailed information on tissue metabolism, whereas planar imaging offers basic functional imaging. These imaging methods, particularly combined with Computed Tomography (CT) to gain anatomical and functional data in a single scan, improve the precision of diagnosis. SPECT/CT and PET/CT are especially beneficial in oncology, neurology and cardiology, where both functional imaging and anatomical localization are crucial for accurate assessment and treatment planning (Alqahtani, 2022).

PET/CT is a more effective method than SPECT/CT for identifying and characterizing lesions because of its greater sensitivity and resolution, which provide superior photon detection (Mohan et al., 2021). Recent developments, such as time-of-flight technology and innovative molecular probes have further enhanced PET/CT performance, allowing for improved lesion differentiation and raising diagnostic accuracy in clinical settings. These clinical applications technologies are growing as they develop, offering important new information about how diseases progress and how well treatments work.

2.1.1 Technetium-99m (99mTC) Radionuclide

Technetium-99m (99mTc) is the most used radionuclide in nuclear medicine mainly for diagnostic imaging. 99mTc is a decay product of Molybdenum-99 (99Mo), which is usually provided using a generator system. This isotope is of particular interest as it emits gamma rays at an energy of 140 keV for detection by gamma cameras and has a short half-life of only 6 hours which means that the patients' uptake of radiation is minimised. These characteristics account for the fact that 99mTc is the radionuclide used for more than 70% of all diagnostic procedures in nuclear medicine including bone, cardiac and oncological applications such as prostate cancer (Boschi et al., 2019). The characteristic of 99mTc to complex with different ligands at oxidation state from +1 to +7 allow to form a wide array of radiopharmaceuticals aimed at specific targets making it very versatile. 99mTc can be used in a variety of diagnostic techniques, such as 99mTc-MAG3 for renal function evaluation (Kelutur et al., 2021). The development of such radiopharmaceuticals relies heavily on the chemical properties of 99mTc, where its coordination chemistry plays a pivotal role in binding to specific biological molecules.

The production of ^{99m}Tc generally involves the use of the ⁹⁹Mo / ^{99m}Tc generator system, where ⁹⁹Mo decays to produce ^{99m}Tc, which is then eluted in the form of sodium pertechnetate (NaTcO₄⁻). This method ensures the ready availability of ^{99m}Tc for clinical use, although the supply chain can be affected by reactor shutdowns, leading to shortages in availability (Boschi et al., 2019). Furthermore, ^{99m}Tc radiopharmaceuticals are created through advanced labeling methods such as the ^{99m}Tc-metal fragment approach, where stable technetium fragments are used to bind bioactive molecules, enhancing the specificity of imaging agents.

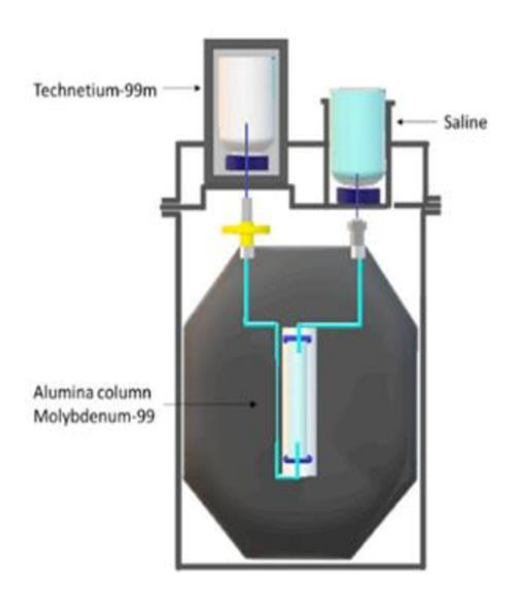


Figure 2.1: Schematic overview of the ⁹⁹Mo/^{99m}Tc generator system. Adapted from Boschi et al., 2019.

2.2 Gamma Camera (SPECT/CT)

SPECT/CT has shown to be a crucial hybrid imaging in oncology, which provides more accurate diagnosis due to the accurate localisation and specification of functional findings (Israel et al., 2019). Recent developments include solid-state detectors based on cadmium-zinc-telluride (CZT) and clinical SPECT cameras with multiple pinhole collimators (Ljungberg & Pretorius, 2018). These developments resulted in increased detection efficiency, better spatial resolution and shorter scanning times. Despite hardware improvements, SPECT reconstruction still requires compensation for photon attenuation, scatter, and collimator response to avoid artifacts and false positives. The clinical benefits of SPECT/CT improved diagnostic accuracy through precise localization and characterization of functional findings, enhancing both sensitivity and specificity. This ensures precise co-registration of anatomic and functional data in a complementary aspect of diagnosis and yields improved evaluation of tumor localization and tumor invasion. Overall, SPECT/CT has paved the way for a broad range of clinical indications in oncology, neurology, cardiology and infection imaging and is still evolving with applications tailor-made for patient care (Bouchareb et al., 2024).

However, there are still some issues remain open in clinical usage of SPECT/CT. One of the significant problems is photon scatter and photon attenuation which affect the quality of SPECT images and might generate false positives (Ljungberg & Pretorius, 2018). These physical limitations must be considered during data processing, despite the advances of the new camera geometries and solid-state detectors. Another problem is the proper registration of SPECT images with CT scans, as it may be hard to align functional and anatomical correlations exactly because patients might move and their organs shift between scans. Although hybrid systems have been developed to minimize patient movement, achieving perfect image registration remains an ongoing challenge. Moreover, the radiation dose is a major issue of SPECT/CT, as the combination of SPECT and CT cause more radiation exposure for the patients. With ongoing advances in the noise reduction techniques including dose modulation techniques and iterative reconstructions, image quality and radiation safety are challenging to maintain a balance. Finally, the high cost of SPECT/CT instruments because of combining SPECT and CT technologies restricts their prevalence in available clinical settings, which may lead to problems of accessibility particularly where other imaging modes such as PET/CT are well spread.

2.3 SPECT/CT Reconstruction

SPECT/CT is the non-invasive imaging methodology for 3D reconstruction of radio-pharmaceutical's distribution inside the body based on 2D measurements. Sophisticated algorithms are used in the reconstruction as the processing faces obstacles of noise, attenuation, and scatter in order to produce high fidelity imaging (Grassi, 2017). Common methods include the Filtered Back Projection (FBP) and Ordered Subsets Expectation Maximization (OSEM). FBP which being a traditional method and computationally faster has been the method of choice for reconstruction, while at the same time, OSEM has gained prominence for its ability to produce higher-quality images, especially in challenging clinical scenarios.

2.3.1 Filter Back Projection (FBP)

FBP is an analytical approach of image reconstruction that contains two main methods which is filtering the projection data to improve high frequency components and then back projecting the filtered data to obtain the image. Filtering is important as it corrects for the intrinsic smoothing in the back-projection stage. Popular filters are the ramp, Hann and Butterworth filters which have characteristic criteria for different imaging needs (Seret & Forthomme, 2009). However, FBP has limitations as in many other widely used methods. It assumes not only perfect data, but also absence of noise, which is unrealistic in a clinical setting. As a result, FBP would generate images with artifacts and low contrast, especially in areas of low tracer accumulation or under conditions of noise. Also, FBP does not inherently account for factors like attenuation and scatter, which can degrade image quality (Seret & Forthomme, 2009).

2.3.2 Ordered Subsets Expectation Maximization (OSEM)

OSEM is an iterative reconstruction algorithm that builds upon the Maximum Likelihood Expectation Maximization (MLEM) framework. It divides the projection data into subgroups and iteratively improves the estimation of the image, leading to a more precise model of the imaging system. Attenuation, scatter, and other compensating corrections for OSEM can also be applied, resulting in better image quality (Cheng et al., 2025). One of the primary advantages of OSEM over FBP is its capability to deal with noisy and incomplete data in a much better way. Study has shown that OSEM yields better imaging quality than FBP particularly in low statistics as it can lower noise and enhance contrast. However, OSEM is more computationally intensive and may not converge easily without carefully optimize the parameters such as the number of the iteration and the subsets, to strike a balance between the image quality and the time of the image processing (Cheng et al., 2025). The optimal number of subsets and iterations in OSEM reconstruction in SPECT depends on many parameters. Byrd et al. (2023) reported that there was an increase in image quality with the use of more iterations (16) and less number of subsets (2)

as compared to the clinical setting (2 iterations 34 subsets), however the processing time was longer. For bone SPECT, Katua et al. (2011) proposed to exploit the bladder-to-acetabulum ratio for parameter decision, in which 4 iterations and 8 subsets would be the optimal choice in most cases. Grassi et al. (2017) emphasized that OSEM update selection depends on object size and desired image quality, noting that fixed parameters are suitable for objects ≥5.5 ml in volume, while smaller objects require careful consideration of partial volume effects.

Both FBP and OSEM have their places in SPECT/CT imaging. FBP offers speed and simplicity, making it suitable for routine imaging where time is critical. On the other hand, OSEM provides enhanced image quality, particularly in challenging cases involving low tracer uptake or noise. The selection between FBP and OSEM should be made based on the need of specific clinical application, local resources and required image quality (Seret & Forthomme, 2009). Between these two reconstruction approaches, OSEM has emerged due to the benefits it offers for enhancing the precision of emission and detection modeling. Attenuation, scatter and collimator detector response corrections are integrated into these algorithms to improve image quality and quantitative accuracy. These corrections are particularly important in applications such as radiopharmaceutical therapy planning in which the accurate quantification of activity is required to assess treatment response. Further investigation will continue to refine these reconstruction methods and enhance the clinical utility of SPECT/CT imaging for a wide range of medical applications, such as dosimetry and tumor localization.

2.3.3 Effects of Different Filter Used

Filters play a crucial role in SPECT image reconstruction, affecting image quality and quantitative measurements. In SPECT, low-pass filters are primarily used to suppress high-frequency noise, while preserving low-frequency signals related to anatomical and pathological features. The filtering process often involves combining a high-pass Ramp filter, which corrects for the blurring intrinsic to back projection, with a smoothing low-pass filter to manage noise

(Lyra & Ploussi, 2011). The key parameters that determine a filter's performance include the cutoff frequency which controls how high-frequency information is retained. For some filters like Butterworth, the order parameter influences the sharpness of the frequency roll-off.

The Butterworth filter is perhaps the most used low-pass filter in clinical SPECT imaging. It is defined by two parameters which are the cutoff frequency and the order. A low cutoff frequency yields smoother images with reduced noise but may blur fine details while a high cutoff enhances detail but also retains noise. Increasing the order results in a steeper roll-off, which can sharpen transitions but may introduce edge artifacts if overly aggressive (Lyra & Ploussi, 2011). Sayed and Ismail (2020) investigated the Butterworth filter's performance using phantom studies and showed that it provides superior image quality compared to the Hamming filter in terms of contrast and region detectability. They tested cutoff frequencies ranging from 0.35 to 0.50 cycles/cm with a fixed order of 7 and found that Butterworth better delineated both hot and cold regions, although signal-to-noise ratio (SNR) decreased with increasing cutoff frequency. This trade-off exemplifies the necessity of application-specific tuning of filter parameters.

The Hamming filter, another low-pass option, is simpler than Butterworth because it only relies on a cutoff frequency. It smooths high-frequency noise effectively, resulting in less grainy images, but generally does not preserve edge detail as well. The Hamming filter showed better SNR preservation at higher cutoff frequencies but at the cost of poorer region detectability and lower contrast values compared to Butterworth (Sayed & Ismail, 2020). The Hann filter functions similarly to Hamming but with slightly different mathematical weighting, resulting in more aggressive high-frequency suppression. While this yields very smooth images with reduced noise, it also risks blurring clinically important features. Lyra and Ploussi (2011) note that the Hann filter is especially effective in whole-body scans or bone imaging, where fine detail is less critical than overall visibility.

The Gaussian filter is characterized by a smooth, bell-shaped response that provides gradual attenuation of high frequencies. Unlike Butterworth or Hann filters, Gaussian filter does not produce sharp frequency cutoffs, which helps avoid artifacts such as ringing or overshoot. It is particularly well-suited for post-processing in iterative reconstruction methods (OSEM), where it reduces background noise without dramatically affecting resolution. Although not the best option for edge preservation, Gaussian filters are often preferred in applications requiring visual smoothness, such as whole-body or tumor imaging. According to Lyra and Ploussi (2011), Gaussian filters also maintain a balance between SNR and contrast, especially when fine structures are not the primary diagnostic concern.

Although digital filters typically function in the frequency domain during or after image reconstruction, the use of physical filters during data acquisition especially in hybrid SPECT/CT systems also impact on image quality. Rana et al. (2015) explored the use of external beam hardening filters made of aluminum (Al) and copper (Cu) to improve CT image quality, which in turn affects the accuracy of attenuation correction maps used in SPECT. By using phantoms filled with iodine contrast and ^{99m}Tc, they evaluated multiple filter thicknesses (1–4 mm) and combinations of CuAl₂. Their findings revealed that 2 mm and 3 mm thick aluminum filters improved uniformity, reduced streak artifacts, and produced higher contrast-to-noise ratios (CNR) in both CT and SPECT/CT images. Copper filters which harder and more attenuating, decreased CNR and increased image distortion due to over filtration. These results demonstrate that physical filters can complement digital filtering strategies by improving the raw data used in image reconstruction (Rana et al., 2015).

The choice of filter type and parameters in SPECT/CT reconstruction plays a pivotal role in image quality, noise control, and diagnostic accuracy. The Butterworth filter remains a robust option due to its tunable parameters, offering a flexible balance between resolution and noise. Hamming and Hann filters provide efficient noise suppression but with some trade-offs in contrast. Gaussian filters offer smooth, artifact-free images and are favored in post-processing

and iterative reconstruction. High-pass filters like Ram-Lak and Shepp-Logan may enhance resolution but require caution due to their susceptibility to noise. Additionally, external beam hardening filters during CT acquisition can indirectly improve SPECT image quality by enhancing attenuation correction. According to Rana et al. (2015), the choice of filter should not be limited to digital algorithms but extended to acquisition hardware as well. Ultimately, filter optimization should be guided by clinical objectives with careful consideration of the imaging system, acquisition parameters and the anatomical region of interest (ROI). Standardization and phantom-based calibration protocols can ensure consistency and improve diagnostic outcomes across imaging centers.

2.4 Activity Quantification of SPECT/CT

SPECT/CT plays a vital role in nuclear medicine as a non-invasive imaging technique used for diagnostic evaluation and therapeutic guidance. Over decades, this modality has increasingly supported not only diagnosis but also applications involving treatment planning through precise assessment of radiotracer distribution and absorbed radiation dose. Crucial to these advances is the absolute quantification of radiopharmaceutical amounts, permitting personalized treatment strategies with known radiation exposure. Recently, feasibility and accuracy have been exhibited for absolute quantification using SPECT/CT. One radiotracer commonly applied is ^{99m}Tc. Phantom studies using diverse radionuclides such as ^{99m}Tc and ¹⁷⁷Lu have measured recovered activity within 10% of actual values. This accuracy has been improved with advanced reconstruction algorithms, hybrid imaging systems, integration of background corrections and volume of interest (VOI) expansion to improve quantification (Bian et al., 2022).

The need for precise quantification of radionuclides is particularly important in radiation therapy planning and monitoring the biodistribution of therapeutic agents. Studies have demonstrated that by improving the VOI and expanding the region to include spill out areas, significant improvements in activity recovery and quantification accuracy can be achieved (Bian

et al., 2022). Nonetheless, several factors such as sphere size, background activity and even patient body mass index can impact the accuracy of quantification (Peters et al., 2019). Intersystem variability also presents challenges with some studies reporting median absolute deviations of up to 16-17% for recovery coefficients across different SPECT/CT systems (Peters et al., 2019). However, standardization of reconstruction protocols can reduce this variability to 4-5%, which can significantly improve the precision of quantification. These advancements in SPECT/CT quantification are key to improving dosimetry calculations and personalized radionuclide treatment planning.

2.4.1 Calibration Factor (CF)

The Calibration Factor (CF) is a fundamental concept in SPECT imaging that translates the raw SPECT counts to the activity concentration. CF is the input conversion factor from the raw counts into a quantitative value used for diagnosis, therapy guidance and monitoring as in nuclear medicine applications. These uncorrected count values for imaging system are not usable in their uncorrected form. The imaging system does not provide direct information about the concentration of the radiopharmaceutical within the body or organ of interest. Hence, imaging has to be calibrated so that imaging data can be used for quantitation (Domenico et al 2023). The CF is often based on use of a phantom containing a known activity of radionuclide. The phantom, whose geometry simulates those of the human body is employed to quantify the activity concentration. The typical CF approval phantoms were tissue equivalent phantoms with uniform cylindrical inserts or homogeneous phantoms with spherical inserts. These phantoms are intended to mimic the body and provide a standard, reproducible environment to evaluate system performance. Calibration is achieved by correlating the measured count rate in the phantom with the known activity concentration, considering the system's sensitivity, photon attenuation, and detector blurring (Ferrando et al., 2018).

For example, according to a standard calibration protocol, a SPECT system capable of imaging ^{99m}Tc will image a uniform cylindrical phantom filled with a known quantity of ^{99m}Tc. The number of counts are determined from a specified ROI in the phantom and activity in the phantom measured dividing the measured counts by the known activity in the phantom. This simple calibration routine is employed to calibrate for quantitative activity concentration. However, the CF is not general and dependent of different factors, such as the phantom geometry, the SPECT/CT system setup and also the collimator type. A high-resolution collimator will result in a different CF than a low-resolution collimator due to difference in spatial resolution and sensitivity. In addition, the size and shape of the imaging area, such as ROI also influences the CF (Domenico et al., 2023).

Standard calibration protocols have been demonstrated to facilitate differences in activity quantification between SPECT/CT systems, making that CF is a crucial element to allow comparison and interpretation of results in different systems. A study by Peters et al. (2019) pointed out that the role of calibration protocols to adjust the systems performance so that regardless of the system configuration, measurement of activity is reliable. The application of CF is more demanded in the case of ¹⁷⁷Lu radionuclide, since even small differences of CF can lead to significant differences in dosimetry calculations and the impact on treatment planning (Ferrando et al., 2018).

2.4.2 Partial Volume Effect (PVE)

Partial Volume Effect (PVE) is one of the most difficult sources of error in SPECT images and especially when imaging small lesions. The fundamental issue arises from the poor spatial resolution of SPECT cameras. Scanning small objects and especially lesions that are less than 2 cm in diameter, results resolution of the accuracy of the activity concentration within the object. This results in spill-out (the activity from the lesion leaks into the surrounding tissue) and spill-in (the activity from the surrounding tissue leaks into the volume of the lesion) effects.

Consequently, smaller lesions systematically receive an underestimation of the activity concentration, possibly causing misinterpretation or incorrect treatment plans (Ferrando et al., 2018).

Phantom studies have shown PVE have a great influence on SPECT accuracy in small lesions. For example, Bian et al. (2022) demonstrated that for spheres with diameters of less than 2 cm, the recovery loss due to PVE is substantial. This recovery loss is largely due to limited spatial resolution of SPECT cameras and can results in significant blurring of activity at the boundaries of small lesions. Partial Volume Correction (PVC) methods are commonly used to correct this influence. PVC is a method to adjust the measured activity concentrations in small ROI by applying the Recovery Coefficients (RC) that are usually obtained from phantom studies. These RC values correct the blurring induced and permit one to retrieve the true radioactivity concentration in the lesion.

A study from Ramonaheng et al. (2021) emphasized the need for PVC in enhancing quantification results of small ROIs. Also, for the SPECT images the activity in small spheres was less underestimated after PVE correction using RC values and therefore of more clinical value. In addition, the PVC correction efficiency also depends on the geometry of the phantom implemented. For instance, sphere-based calibration has been found to yield better results compared to cylinder-based calibration where the lesions are spherical in shape, which is often the case in clinical imaging of tumors (Ramonaheng et al., 2021).

2.4.3 Recovery Coefficient (RC)

Recovery Coefficients (RC) are used to correct the measured activity concentration considering the PVE in small lesions. These factors are determined from phantom measurements in which spheres of different diameters are filled with known activities of radiopharmaceutical and activity concentration is measured in the ROI. RC is defined as the measured activity concentration in the phantom divided by the true activity concentration. RC values is important

since they can be used to correct the activity loss associated with the limited spatial resolution of the SPECT camera, thereby to avoid inaccurate quantification of small lesions (Ferrando et al., 2018).

In recent studies, it has been observed that smaller lesions (less than 2 cm in diameter) are particularly susceptible to underestimation due to PVE. Small lesions have smaller RC than large lesions because the loss of activity in small probe hot spots caused by the blur is greater. The RC values are affected by the reconstruction algorithm. For instance, the use of iterative reconstruction algorithms (OSEM) may markedly improve the accuracy of small lesion quantification by minimizing the effect of poor resolution and low recovery. The use of these sophisticated algorithms has been demonstrated to increase the accuracy of PVC and thus the accuracy of small lesion quantitation.

For example, the study by Giovanni Di Domenico et al. (2023) demonstrated that the utilization of RC values obtained from phantom studies in ¹⁷⁷Lu SPECT imaging resulted in a better accuracy of activity quantification for small lesions as well as organ-oriented (liver and kidneys) applications. When PVC was performed using these RC factors, the activity concentration in small lesions was much better estimated, resulting in better input data for the dosimetry estimation. The application of RC values from homogenous phantoms was particularly advantageous with respect to quantification accuracy in complex organs such as the kidneys.

The importance of using geometry-specific RC has also been increasingly emphasized, as has been done in several studies focusing on precise tumor localization and tumor monitoring. These studies emphasize that the application of RC when combined with PVC techniques, plays a critical role in mitigating the errors that arise due to the PVE. These errors, arising predominantly from the finite spatial resolution of the imaging device, can introduce underestimation or misinformation of small lesions. By combining RC with PVC, the system is more sensitive to these distortions, leading to a more accurate measurement of the actual activity inside the tumors. Thus, the use of such techniques serves to reduce errors while simultaneously

ensuring a more reliable data set for tumor localization. This enhanced imaging precision is particularly important in SPECT/CT imaging since it is the basis for individualized treatment plans. The ability to more accurately localize the tumor allows clinicians to tailor treatment regimens based on the patient's individual anatomical and physiological characteristics rather than the entire population of patients with a similar type of cancer, thereby increasing the effectiveness of treatment, minimizing treatment risks and improving the potential for positive clinical outcome.

2.4.4 Spatial Resolution

Among the factors affecting quantitative reliability, spatial resolution is most important in SPECT. Poor spatial resolution can cause the images to be blurred images, making it difficult to distinguish between adjacent structures. This is especially problematic in small lesion detection where activity spill-out can cause significant errors in quantification. Nevertheless, technological advances in SPECT/CT systems, especially in the incorporation of CT-based attenuation correction (CTAC) and iterative reconstruction methods have contributed to the increase in the resolution. CTAC is recognized as one of the essential procedures for enhancing spatial resolution in SPECT/CT imaging. CT data is used as an attenuation map for correcting for loss of photons due to absorption in tissue. This correction increases the contrast and sharpness of SPECT images and hence improves the accuracy of activity quantification, especially for small lesions (Peters et al., 2019).

Apart from the standard attenuation correction (AC), Evidently, it has been well recognized that the OSEM reconstruction is very essential to provide substantial enhancement of the spatial resolution of SPECT/CT images while suppressing image noise levels. This improved resolution, combined with improved activity recovery is necessary to increase spatial detail and accuracy of quantitative estimates. The OSEM algorithm is widely implemented in many current imaging systems and considers several advanced techniques including scatter

correction and resolution recovery, the two physics-based models which are crucial for enhancing the quality in terms of sharpness and clarity of the images. Scatter correction reduces the influence of scattered photons which can degrade image quality and resolution recovery corrects for the fact that the spatial resolution of the imaging system is inherently limited, so that small details in the image do not disappear (Saffar et al., 2013).

However, there are some pros and cons to the gains in spatial resolution. Needing more computational resource for processing and more time for computation is a challenging problem particularly in a clinical setting where the time that can be granted and the computational power that may be requested are both generally very limited. Therefore, a balance must be achieved between maximizing the spatial resolution and allowing for computational efficiency. This tradeoff is important to be able to produce efficient images of good quality without the needlessly increasing of the processing time, where the advantages of superior image resolution do not act in a such way at the expense of practical usefulness in real-world clinical settings.

In summary, CF, PVE and RC are all essential factors to consider in accurate SPECT imaging. The CF allows the raw imaging counts to be transformed into clinically useful activity concentrations and the PVC and RC provides the correction for errors caused by PVE especially in small lesion. Recent studies results underline the need for phantom based calibrations and reconstruction algorithms to improve SPECT quantification accuracy, in particular for small lesions, which are most frequently of clinical relevance. Through using geometry specific RC and optimizing the reconstruction parameters such as OSEM, the accuracy of tumor localization and monitoring with SPECT/CT may be improved dramatically. These calibration and calibration related developments are essential to the move towards patient specific dosimetry and so are contributing to an improved efficacy of nuclear medicine with respect to patient outcome.

CHAPTER 3

METHODOLOGY

3.1 Material

This research was carried out at the Department of Nuclear Medicine, Radiotherapy and Oncology, Hospital Pakar Universiti Sains Malaysia. Several materials and equipment are used in this study including GE Discovery NM/CT 670 Pro SPECT/CT gamma camera for scanning the phantom and NEMA 2007/IEC 2008 phantom which is used to test imaging systems. It is applied to check the functionality of the system using a ^{99m}Tc pertechnetate source. A 25-cc syringe and plastic tube is used to insert the source into six different sizes of spherical vials within the NEMA phantom, ensuring accurate placement for each sphere. For ^{99m}Tc source activity measurements, a well-type ionization chamber dose calibrator (AtomlabTM 500) is used. Acquisition and registration of images registration and acquisition were performed on the Xeleris workstation to reconstruct high quality images for analysis. The quantitative analysis of resolution was then carried out using Q Metrix software, which is used to calculate the recovery coefficient (RC) value for each sphere and background, providing valuable data on the gamma camera's performance and the accuracy of imaging across different sphere sizes.

3.1.1 Discovery NM/CT 670 Pro SPECT/CT

At HPUSM, the Discovery NM/CT 670 Pro SPECT/CT machine from GE Healthcare is used to enhance clinical diagnosis through its integration of both SPECT and CT technologies. This advanced hybrid imaging technology comprises a dual-head gamma camera with a 70 cm gantry diameter and is capable of performing H-mode and L-mode. The dual-head gamma camera of this system is a high-energy collimator with a 70 cm gantry and can be placed in H-mode or L-mode. The camera enables the acquisition of the anterior and posterior projections simultaneously or separately and can be used to make whole-body planar and gated SPECT

acquisitions. It may also be combined with other multi-slice CT evaluations. The camera features interchangeable collimators including Low Energy General Purpose (LEGP), Low Energy High Resolution (LEHR), Medium Energy General Purpose (MEGP), and High Energy General Purpose (HEGP). Selection of a proper collimator is based on the energy of the radionuclide used, the purpose of the scan, and the patient's region of interest (ROI). With a dual-head variable-angle and a 16-slice CT configuration, the Discovery NM/CT 670 Pro provides faster imaging and advanced gantry robotics for accurate multi-axis positioning. Studies have found significant differences in how SPECT/CT imaging is performed, leading to suggestions for improving these practices. Recommendations include setting diagnostic reference levels and taking actions to optimize the process, ensuring patient safety while maintaining high diagnostic quality (S. Avramova-Cholakova et al., 2015).



Figure 3.1:GE Discovery NM/CT 670 Pro SPECT/CT used at HPUSM

3.1.2 **NEMA 2007/IEC 2008 Phantom**

The NEMA 2007/IEC 2008 phantom used in this study is a standardized imaging phantom designed for the calibration and performance testing of SPECT/CT scanners. It includes several components aimed at simulating human anatomy and providing accurate representations

of different tissue types. This phantom is equipped with a lung insert, a body phantom and an insert containing six different-sized spheres. The lung inserts mimic the attenuation and density of lung tissue, while the body phantom represents the soft tissues. Table 3.1 below shows dimension of NEMA phantom used in this study.

Table 3.1: The dimension of NEMA phantom used in this study

Component	Dimension
Height	24.1 cm
Width	30.5 cm
Depth	24.1 cm
Cylindrical Insert	51 mm diameter x 180 mm length
Spheres (Inner Diameter)	10 mm, 13 mm, 17 mm, 22 mm, 28 mm, 37 mm

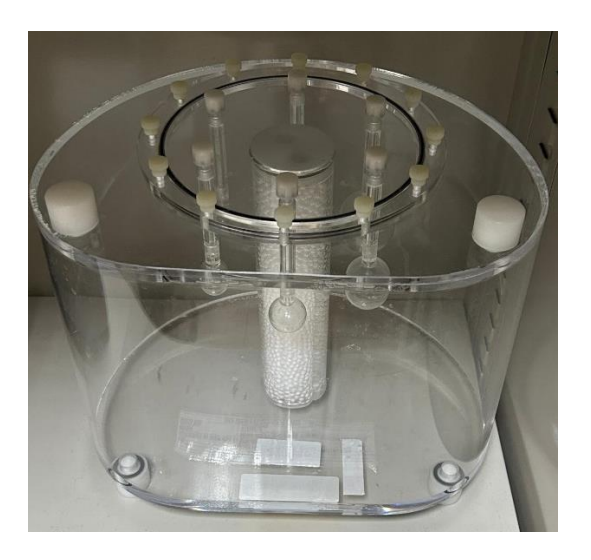


Figure 3.2: NEMA 2007/IEC 2008 phantom

This phantom also includes six fillable spheres with each having different inner diameter, which are designed to simulate lesions or abnormalities at various sizes within the body. These spheres placed inside the phantom to allow for accurate imaging and performance testing of the scanner's ability to detect small structures at varying depths. The volume of the empty space within the phantom is 9.7 liters (Mirion, 2025). Table 3.2 below shows detailed dimensions of six spherical shapes in NEMA phantom.